Metallo-supramolecular coordination polymers based on amidopyridine derivatives of pillar[5]arene and Cu(II) and Pd(II) cations: synthesis and recognition of nitroaromatic compounds

*Dmitriy N. Shurpik,[†] Yulia I. Aleksandrova,[†] Alexander A. Rodionov,[‡] Elena A. Razina,[‡] Marat R. Gafurov,[‡] Vakhitov I. Rashidovich,[‡] Vladimir G. Evtugyn[††], Alexander V. Gerasimov,[†] Yurii I. Kuzin,[†] Gennady A. Evtugyn,[†] Peter J. Cragg [‡†] and Ivan I. Stoikov [†]**

[†]A.M.Butlerov Chemical Institute, Kazan Federal University, 420008, Kremlevskaya Street, 18, Kazan, Russian Federation

[‡] Institute of Physics, Kazan Federal University, Kremlevskaya, 18, Kazan 420008, Russia.

[††] Interdisciplinary Centre for Analytical Microscopy, Kazan Federal University, 420008 Kazan, Kremlevskaya 18, Russian Federation.

[‡†] School of Pharmacy and Biomolecular Sciences, University of Brighton, Huxley Building, Moulsecoomb. Brighton, East Sussex BN2 4GJ, UK.

KEYWORDS: pillar[5]arene, self-assembly, SEM, MOF's, macrocyclic receptors.

Decasubstituted pillar[5]arenes containing amidopyridine fragments have been synthesized for the first time. As was shown by UV-Vis spectroscopy, the pillar[5]arenes with p-amidopyridine fragments form supramolecular associates with Cu(II) and Pd(II) cations in methanol in 2:1 ratio. These associates are transformed into metallo-supramolecular coordination polymers (supramolecular gels) using a sol-gel approach which were characterized as amorphous powders by scanning electron miscroscopy (SEM) and dynamic light scattering (DLS). The powders are able to selectively adsorb up to 46% of nitrophenols from water and were incorporated into an electrochemical sensor to selectively recognize them in aqueous acidic solution.

Introduction

The modern concept of supramolecular chemistry has been recently transformed from investigations of simple supermolecules to polymacromolecular systems capable of self-organization and molecular recognition. [1] Among others, metallo-supramolecular coordination polymers [2] based on non-covalent interactions are of special interest. [3] Metal–ligand coordination is a convenient approach for assembling of supramolecular systems as it allows control over structure through highly directional coordination bonds together with thermodynamic and kinetic stability through selectivity of appropriate types of ligands and metal ions. [2] Such materials exert attractive properties such as electrochromism,[4] fluorescence[5] and chemosensory applications.[6]

The ability of metallo-supramolecular coordination polymers to selectively recognize organic molecules in solution and at the solid-liquid interface has been investigated intensively.[7, 8]

Nitroaromatic compounds are frequently encountered due to their wide application as explosives, pharmaceuticals, industrial solvents and auxiliary compounds of organic synthesis.[9, 10] Thus, the development of effective methods for their detection and selective extraction is necessary to protect both the population and the environment.

To date, many metallo-supramolecular coordination polymers have been developed to analyze and/or extract nitroaromatic compounds.[11 – 14] However, they have common disadvantages including complex synthesis, poor functionality and insufficient thermodynamic stability. The use of macrocyclic compounds as ligands in the assembling of the metallo-supramolecular coordination polymers removes some of these drawbacks.[5, 15] For example, molecular recognition occurs within macrocyclic cavities rather than voids in the coordination lattice and their spatially pre-organized functional groups are also useful for creating structurally ordered polymers. [5, 15] In the literature, metallo-supramolecular coordination polymers based on functionalized calixarenes, [16] cyclodextrins, [17, 18] cucurbiturils,[19] pyrogallol[4]arenes,[20] and cyanostar [21] have been described. The introduction of the functional groups in the above systems can be rather complex, time- and labor-consuming so, as an alternative to these macrocyclic platforms, we propose assembling metallo-supramolecular coordination polymers from a new class of *para*-cyclophanes, the pillar[5]arenes.[22, 23] Pillar[5]arenes are synthetically accessible, easily functionalized macrocycles with tubular structures ideal for host-guest complexation and self-assembly. [24 – 28]

Although pillar[5]arenes consist of the hydroquinone fragments that are electrochemically active, few works have been devoted to their redox behavior and application as electrochemical sensors although the similarity of redox behavior of pillar[5]arene to that of hydroquinone was demonstrated by direct current voltammetry.[29] In aqueous solution, pillar[5]arene undergoes stepwise oxidation with intermediate formation of quinhydrone structures.[30] The reaction is

complicated by chemisorption on bare glassy carbon [29] and non-covalent aggregation on the electrode modified with carbon black particles.[30] Weak acids affected the aggregation due to the shift of the equilibria of hydrogen bonding and hence altered the redox activity of the macrocycles.[30] This effect was used for the voltammetric detection of organic acids and discrimination of native and oxidatively or thermally damaged DNA. Redox properties of pillar[5]arene were utilized to determine acetylcholinesterase inhibitors [31] and antioxidants. [32]

In this work, for the first time we report the application of decasubstituted pillar[5]arenes containing amidopyridine fragments as ligands which assemble into metallo-supramolecular coordination polymers with Cu^{2+} and Pd^{2+} cations and demonstrate their use in electrochemical sensors to detect nitroaromatic compounds.

Results and Discussion

We have previously shown [33] that decacid **1** can be converted to the acid chloride in quantitative yield in the presence of thionyl chloride. Thus, decacid **1** was converted to the acyl chloride derivative of macrocycle **1** by thionyl chloride in the presence of catalytic amounts of DMF, which was involved *in situ* in the reaction with an excess of 2-, 3-, 4-aminopyridine at a reduced temperature in anhydrous methylene chloride over 72 hours. An excess of the corresponding aminopyridine acted as an effective base.[34] Introduction of amidopyridine fragments in the structure of a pillar[5]arene sufficiently increases the affinity of the macrocycle for d-metal cations due to complementary interactions in accordance with Pearson's soft acid - soft base theory. As a result, stable coordination complexes are formed due to the presence of the σ-donating N-amido groups. This promotes stabilization of the metal ions in their high oxidation state.[35] The target

products were isolated by recrystallization from water. Macrocycles **2-4** were isolated in 77%, 61% and 71% yields, respectively (Figure 1).

One-dimensional ^{1}H and ^{13}C NMR, IR spectroscopy and mass spectrometry confirmed the structures of products **2-4** and their compositions were confirmed by elemental analysis data (ESI, S2-S9).

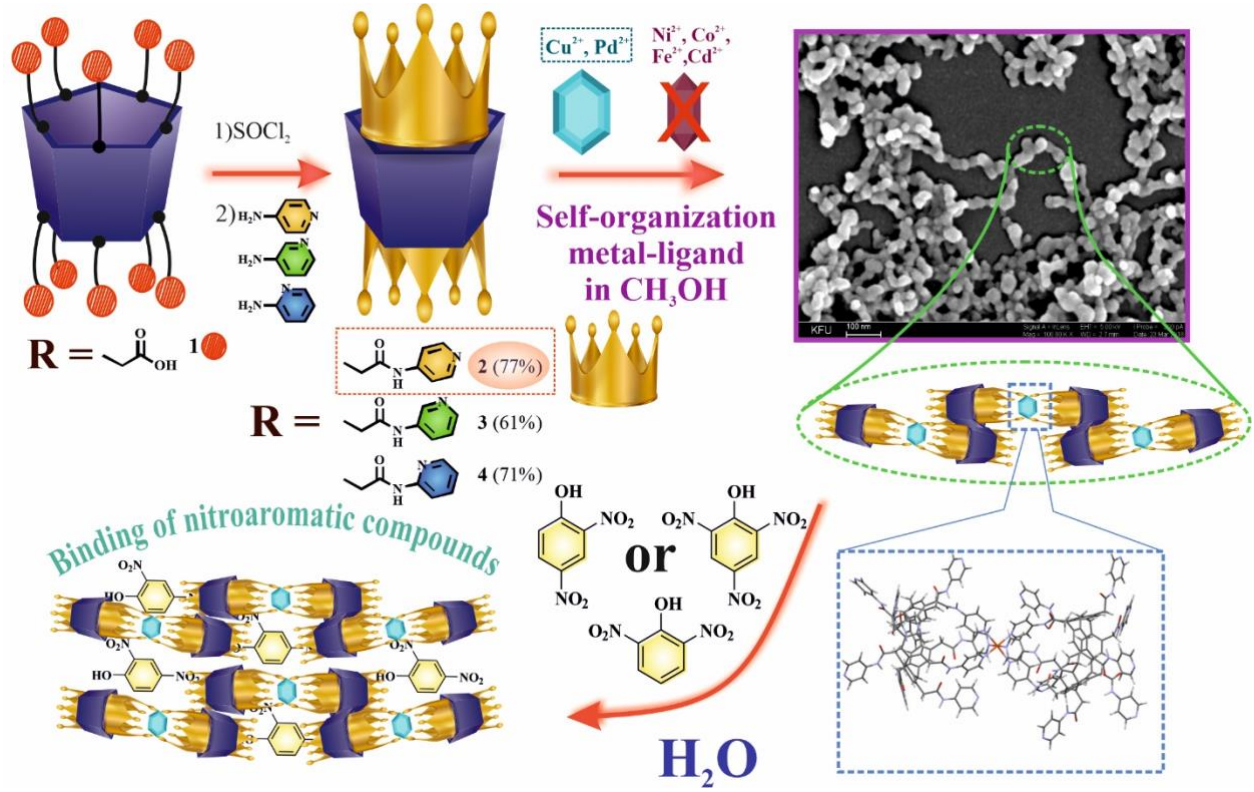

Figure 1. Synthesis of the macrocycles **2-4**: the sketch represents the proposed structure of metallo-supramolecular complex **2**/Cu^{2+} or **2**/Pd^{2+} by self-organization, as determined by molecular mechanics (MMFF), and the molecular recognition of nitrophenol derivatives by **2**/Cu^{2+} or **2**/Pd^{2+}.

Self-aggregation of pillar[5]arene derivatives and their interactions with the d-metal cations

The self-association of the macrocycles **2**-**4** and their aggregation with the metal cations (Cu^{2+}, Fe^{2+}, Ag^{+}, Ni^{2+}, Co^{2+}, Cd^{2+}, and Pd^{2+}) has been investigated. The choice of the *d*-metals was made based on their frequent application in the synthesis of the metallo-supramolecular coordination polymers.[7] The investigations were performed in methanol and dichloromethane by DLS. Compounds **3** and **4** were insoluble in methanol so that their self-association process was investigated only in dichloromethane. Incorporation of ten *p*-amidopyridine fragments in compound **2** increased its solubility and resulted in formation of homogeneous solutions both in methanol and dichloromethane. When dissolved, macrocycle **2** formed self-associated structures at concentrations from 1.0 mM to 10 μM but only in methanol.

Macrocycle **2**, at 0.1 mM in methanol, self-assembled into monodisperse associates with a hydrodynamic diameter of 120.5 nm and the polydispersity index (PDI) of 0.12 (ESI, S21). As shown in TEM images of the self-associates formed by macrocycle **2**, they exist as oval particles with an average length of 150 nm and width of 40 nm (Figure 1, ESI, S23). No associates of macrocycles **3** or **4** were observed under the same conditions in dichloromethane. It is obvious that the formation of intermolecular hydrogen bonds, in the case of macrocycles **2-4**, should lead to the formation of associates. Amide (-C (O) -NH-) groups can act as proton donors in macrocycles **2-4**, and carbonyl (-C (O) -) groups and nitrogen atoms of pyridine fragments act as proton acceptors. The nature of the substituents and the spatial structure of macrocycles **3** and **4** allow the formation of intramolecular hydrogen bonds. The formation of intramolecular hydrogen bonds is observed by the shifts of the vibrations band of the amide bond in the IR spectrum of macrocycle **2**. Thus, the bands Amide 1 (1703 cm^{-1}) and Amide 2 (1598 cm^{-1}) of macrocycle **2** are shifted to the high-

frequency region as compared to the vibration bands of macrocycles **3** and **4** (Amide 1 (1698 cm^{-1}), Amide 2 (1576 cm^{-1}), ESI, S10). The location of the nitrogen atom in positions 2 and 3 of the amidopyridine ring leads to deactivation of pyridine coordination centers and prevents association processes. The nitrogen of the amidopyridine ring of macrocycle **2** is located at position 4, which prevents the formation of intramolecular hydrogen bonds and leads to the formation of supramolecular associates. The oval shape of the associates is the most thermodynamically favorable shape.

Then, the reaction of decasubstituted macrocycles **2**-**4** containing pyridine fragments with *d*-metal cations (Cu^{2+}, Fe^{2+}, Ag^{+}, Ni^{2+}, Co^{2+}, Cd^{2+}, and Pd^{2+}) in methanol and dichloromethane was monitored using UV-vis spectroscopy. According to UV-vis spectroscopy data, interactions of Cu^{2+}, Fe^{2+}, Ag^{+}, Ni^{2+}, Co^{2+}, Cd^{2+}, Pd^{2+} ions with macrocycles **3** and **4** in the dichloromethane/methanol (100/1) system was not observed. However, for macrocycle **2**, there was an interaction in the presence of Cu^{2+} and Pd^{2+} in methanol. Thus, three bands appeared in the UV-vis spectrum of the macrocycle **2** in the absence of the metal cations at 287, 244 and 210 nm. The bands corresponded to the *n*-π transfer of the electrons of the aromatic system, the pyridine ring and the amide group. [36] The band at 244 nm exerted a bathochromic shift to 267 nm in the presence of Pd^{2+} ions (ESI, S11) and to 257 nm in the presence of the Cu^{2+} ions (Figure 2a, ESI, S11). New bands appeared at 267 and 257 nm corresponded to the formation of new coordination metal (Cu^{2+} and Pd^{2+}) – ligand **2** bonds.[37]

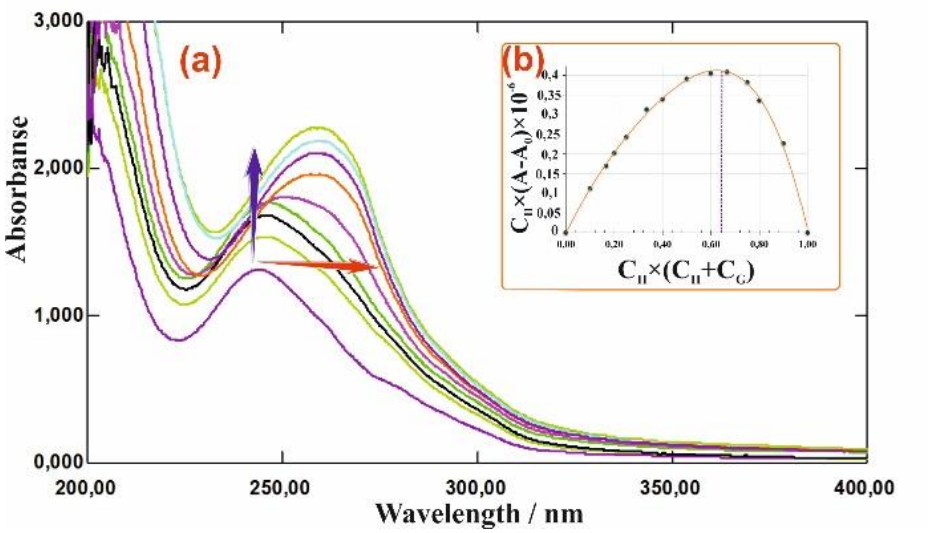

Figure 2. (a) UV-vis spectra of the macrocycle **2** (10 μM) at different concentrations of Cu^{2+} ions; (b) Job's plot for the complex of Cu^{2+} ions with the macrocycle **2**.

The association constant of the complex **2**/Cu^{2+} was established by spectrophotometric titration at 257 nm and found to be 10^{-5} M in the range of the cation concentration from 2.5 to 90 μM and constant ligand concentration (10 μM). The logarithm of the association constant was equal to 4.91 (ESI, S11). The stoichiometry of complex formation was assessed using an isomolar series (Job's method) and found to be 2:1 for the macrocycle **2**: Cu^{2+} (Figure 2b). Additional results have been obtained by the analysis of the binding isotherms with the BindFit software [38, 39] adapted to the 2:1 binding model (ESI, S12). The association constant for the binding of the macrocycle **2** to Cu^{2+} was estimated as $K_{1:1}$ = 17 M^{-1} and $K_{1:2}$ = 113170 M^{-1}. Similar estimations for the host: guest binding models 1:1 and 2:1 were inappropriate because of too high error of the constant calculation (ESI, S12).

Similar behavior was found for the electron absorbance spectra corresponded to the association of the macrocycle **2** with the Pd^{2+} ions in methanol giving log K_a = 5.97 based on a 2:1 stoichiometry (ESI, S11). The BindFit assessment for the 2:1 binding model confirmed the above parameters

($K_{1:1}$ = 28 M^{-1}, $K_{2:1}$ = 9827072 M^{-1} (ESI, S13). It should be noted that increased concentration of the **2**/Cu^{2+} and **2**/Pd^{2+} in methanol from 10 μM to 1.0 mM was followed by significant rise of the baseline in the UV-vis spectra indicating higher light scattering because of the aggregation processes.

Formation of the metallo-supramolecular coordination polymers

Light scattering methods mentioned in the previous section made it possible to conclude that all ten *p*-amidopyridine fragments of macrocycle **2** could be involved in the formation of metallo-supramolecular coordination polymers based on the non-covalent interactions with bridging Cu^{2+} or Pd^{2+} ions. To prove this suggestion, the systems **2**/Cu^{2+} and **2**/Pd^{2+} were investigated by DLS with the reactants in ratios of 10:1, 5:1, 2:1, 1:1, 1:2, 1:5, 1:10 from 1.0 mM to 10 μM. Only the **2**/Cu^{2+} complex obtained in a 2:1 ratio from a 0.1 mM ligand solution formed monodisperse stable associates (ζ=+33.4 mV) with an average hydrodynamic diameter of 80 nm (PDI = 0.23) (ESI, S23). For the **2**/Pd^{2+} system, stable associates (ζ=+30.1 mV) were found for the same stoichiometry and concentration of reactants and had a hydrodynamic diameter of 66 nm (PDI = 0.19) (ESI, S22). Increase of the ligand concentration to 1.0 mM and changes in reactant ratios to 1:5, 1:10, 5:1, or 10:1 resulted in higher diameters of aggregates of **2**/Cu^{2+} and **2**/Pd^{2+} though the PDI value sharply increased. At the concentration of the mixtures of **2**/Cu^{2+} and **2**/Pd^{2+} (2:1) equal to 10 mM, metallo-supramolecular coordination polymers were formed as supramolecular gels. The gel structure of **2**/Cu^{2+} and **2**/Pd^{2+} was confirmed by optical microscopy (Figure 3a and 3b).

As can be seen on Fig. 3a for **2**/Cu^{2+} and Fig. 3b for **2**/Pd^{2+}, illuminated areas (the halo effect) were observed on the gel surface in the dark field reflected light mode (DFRL).[40] This phenomenon resulted from heterogeneity and roughness of the surface with various thicknesses of the layer and

from the lack of crystallinity in the structure of the supramolecular associates (**2**/Cu^{2+} and **2**/Pd^{2+}).[40, 41] The gel structure was also confirmed by TEM. Contrary to the oval-like self-associates of macrocycle **2**, TEM images of the associates **2**/Cu^{2+} (Figure 3c and 3d) and **2**/Pd^{2+} (Figure 3e and 3f) showed that the structure of the gel matrix consisted of a regular dense 3D net of nanofibers with a filament diameter of ca. 20 nm in case of **2**/Cu^{2+} system and 30 nm for **2**/Pd^{2+} system. These systems could not be studied by NMR spectroscopy because gelation was observed at low concentrations of reactants (0.1 – 10 mM).

Based on the experimental data obtained, a mechanism explaining gelation process can be proposed by which Cu^{2+} and Pd^{2+} cations form hexa-coordinated complexes with pyridine fragments of macrocycle **2**. Combining a number of these heterocycles into a chain leads to the formation of the nanofibers of the metallo-supramolecular coordination polymer. [42]

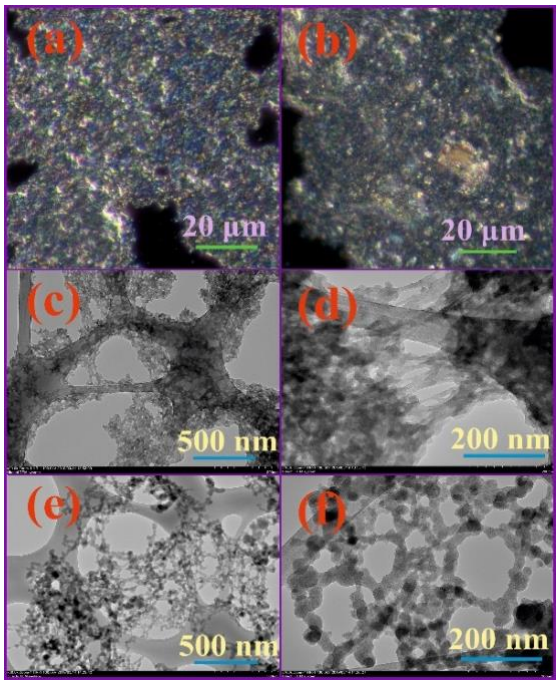

Figure 3. DFRL images: (a) **2**/Cu^{2+} (10 mM) in CH_3OH; (b) **2**/Pd^{2+} (10 mM) in CH_3OH. TEM images: (c) and (d) system **2**/Cu^{2+} (5×10^{-4} M) in CH_3OH; (e) and (f) system **2**/Pd^{2+} (5×10^{-4} M) in CH_3OH.

Due to a large size of the Cu^{2+} and Pd^{2+} cations, they are positioned outside the macrocyclic cavity.[43] Amide bonds in the structure of macrocycle **2** promote the formation of additional hydrogen bonds between the nanofibers.[44] This results in assembling of a regular gel structure as a dense 3D net. However, the regular gel structure can be destroyed depending on the microenvironment conditions, e.g., temperature shift, solvent substitution etc., which limits working conditions for particular gels.

Sol-gel methods were used to preserve the regular structure of the metallo-supramolecular coordination polymers **2**/Cu^{2+} and **2**/Pd^{2+}. This approach did not require high temperature or pressure [45] to transform gels into stable powders. This made it possible to obtain porous metallo-supramolecular coordination polymers **2**/Cu^{2+} and **2**/Pd^{2+} as amorphous powders. The structure of the obtained polymers **2**/Cu^{2+} and **2**/Pd^{2+} was studied by PXRD (ESI, S26). The amorphous structure of the metallo-supramolecular coordination polymers **2**/Cu^{2+} and **2**/Pd^{2+} was proved by a lack of diffraction. No intense crystallographic reflections were observed and the diffractograms of **2**/Pd^{2+}, **2**/Cu^{2+} differed little from that of macrocycle **2**. The peak for bonded Pd^{2+} in diffractogram of the **2**/Pd^{2+} at $2\theta = 40^{o}$ confirmed the existence of palladium in the polymer.

The stability of the metallo-supramolecular coordination polymers **2**/Cu^{2+} and **2**/Pd^{2+} were investigated by FTIR spectroscopy after solvent removal. Similar characteristic bands of the main functional groups were present in the range from 940 to 1850 cm^{-1} in the IR spectra of **2**/Cu^{2+} and **2**/Pd^{2+} polymers (ESI, S10). In comparison with the spectrum of macrocycle **2**, the absorbance band at 1650 cm^{-1} attributed to the pyridine ring vibrations, disappeared and one additional band consistent with vibrations from the bonded NH group (1590 cm^{-1}) appeared (ESI, S10). The results obtained correspond to the literature data [46] and prove the hypothesis on the possible assembling

of the metallo-supramolecular coordination polymers on the base of the macrocycle **2** and *d*-metal cations.

The synthesized metallo-supramolecular coordination polymers **2**/Cu^{2+} and **2**/Pd^{2+} were studied using TGA-DTA/DSC (ESI, S25). As was shown, the polymers **2**/Cu^{2+} and **2**/Pd^{2+} were stable up to 270 °C for **2**/Cu^{2+} and 320 °C for **2**/Pd^{2+}. Loss of organic mass during thermal decomposition was 74.74% for **2**/Pd^{2+} and 78.65% for **2**/Cu^{2+}. The results obtained coincide well with theoretically calculated loss of the aggregate mass for **2**/Pd^{2+} (73.35%) in accordance with the 1:4 stoichiometry of the **2**/Pd^{2+} complex. For **2**/Cu^{2+}, mass loss calculated (76.74 %) corresponds to the 1:2 stoichiometry of the complex.

The morphology of the metallo-supramolecular coordination polymers **2**/Cu^{2+} (Figure 4a) and **2**/Pd^{2+} (Figure 4b) was studied with SEM. The SEM images (Figure 4a and 4b) indicated that the structure of regular dense 3D net of polymeric nanofibers had been retained for both **2**/Cu^{2+} and **2**/Pd^{2+} polymers. The presence of palladium, carbon and nitrogen in the structure of the **2**/Pd^{2+} was confirmed by EDS mapping (Figure 4c, ESI, S24). Application of the EDS mapping for **2**/Cu^{2+} was impossible because of high level of copper in the underlying surface material.

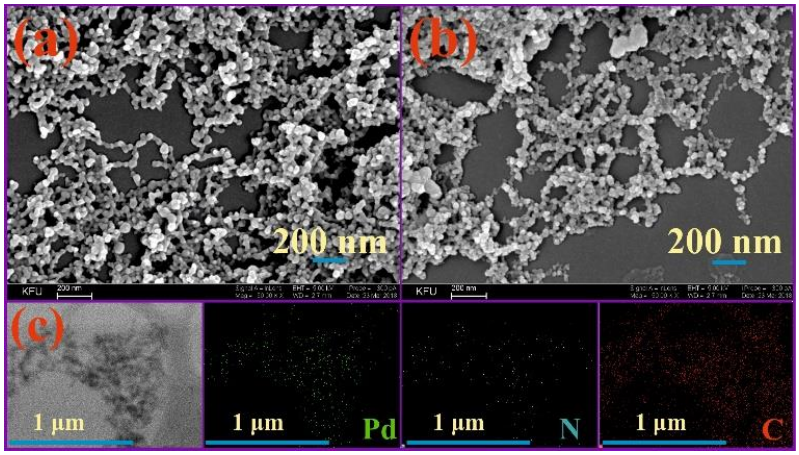

Figure 4. SEM images: (a) **2**/Cu^{2+}; (b) **2**/Pd^{2+}; (c) EDS mapping of Pd, N, and C, respectively.

To evaluate the spatial structure of the obtained polymer **2**/Cu^{2+} containing paramagnetic centers and to prove the existence of coordinated copper, electron paramagnetic resonance (EPR) was applied. It should be noted that EPR allows the structure of coordination center with paramagnetic metal atom to be established. EPR can operate with liquid and solid samples in a wide range of temperature and hence is suitable for the investigation of the metallo-supramolecular coordination polymers.[47,48] EPR spectra were recorded for the 50 μM aggregate **2**/Cu^{2+} at 20-100 K (Figure 5b) and for the powder of the **2**/Cu^{2+} polymer in the range from 100 to 270 K (Figure 5a).

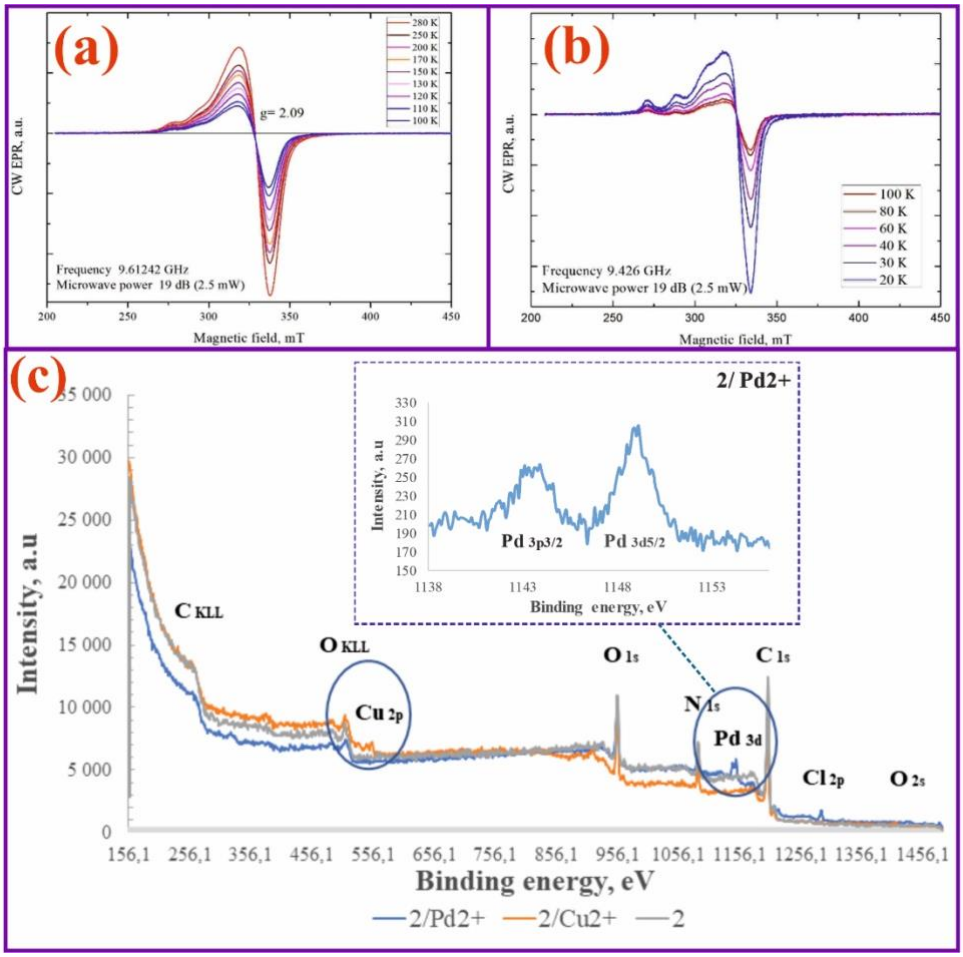

Figure 5. EPR spectra: (a) polymer powder **2**/Cu^{2+} in the temperature range 100-270 K; (b) polymer solution of **2**/Cu^{2+} (50 μM) in the temperature range of 20-100 K.; and (c) XPS survey spectra of 2/Cu^{2+} and 2/Pd^{2+}.

The EPR experiments showed the coordinated Cu in the **2**/Cu^{2+} system both in liquid and solid phase. The intensity of the EPR spectrum decreased inversely to the temperature ($I \propto A/T$) with no deviation from the Curie's law. This observation testifies that no phase transfer occurred in the **2**/Cu^{2+} system and the absence of paramagnetic centers other than copper over the temperature range from 20 to 300 K. The powder spectra of the metallo-supramolecular coordination polymer **2**/Cu^{2+} (Figure 5a) and of the solution of the **2**/Cu^{2+} aggregate (Figure 5b) are identical. This confirms that the spatial organization of the copper ions both in the powder and complex solution is similar. [49]

The EPR spectra are characterized by the values of *g*-factor (as an analog of the Landé spectroscopic splitting factor that makes it possible to conclude about the orbital structure of the molecule studied) and hyperfine structure of interaction of electronic spin with the neighboring nuclei (both stable isotopes ^{63}Cu and ^{65}Cu have nuclear magnetic spin $I = 3/2$), described by the components of parameter A. This, and the known anisotropies of the spectroscopic parameters g and A for Cu^{2+} in different matrices, directly allows the assignment of the spectra presented in Figure 5 to Cu^{2+} due to 4 lines detected at $g_z \approx 2.3$-2.4 at low temperatures.[50]

Thus, the following anisotropic parameters of the EPR spectra of the aggregate **2**/Cu^{2+} were determined: $g = [2.08; 2.14; 2.32]$, $A = [10; 90; 570]$ MHz, assuming that the main axes of *A*- and *g*-tensors coincide (These quantities depend on the mutual orientation of the field and the intrinsic crystallographic axes of the molecule. They reflect the properties of the local symmetry of the paramagnetic center and characterize the local symmetry of the wave function near interacting nuclei). It suggests an almost axial geometry for the complex with two values of the *g*- and A-tensors:[51] $(g_{\perp} = (g_{xx} + g_{yy})/2 \approx 2.11$; $A_{\perp} = (A_{xx} + A_{yy})/2 \approx 50$ MHz, $g_{\parallel} = g_{zz} = 2.32$, $A_{\parallel} = A_{zz} = 570$ MHz. Because $g_{xx} \approx g_{yy} < g_{zz}$, the EPR spectra (Fig. 5a, b) contain signals in high fields and

intensive peaks as the Lorentz curve is in a low field area.[52, 53] The characteristics obtained agree with the literature data [54, 55] on six-coordinated copper being is elongated along d_{z2} axis due to Jahn-Teller distortion of the d^9-species and may indicate interactions with two different types of ligands. It is suggestive (Fig. 1) of four pyridine ligands are positioned in equatorial plane of the metal and two nitrate groups in axial plane.

The elemental composition, oxidation state of elements of macrocycle **2** and polymers **2**/Cu^{2+}, **2**/Pd^{2+} were measured by X-ray photoelectron spectroscopy (XPS) (Fig. 5c, ESI, S20-S21). The XPS spectra of metal-organic polymers **2**/Cu^{2+}, **2**/Pd^{2+} show peaks of metal elements (Cu, Pd), which indicates successful cross-linking of metals with macrocycle **2**. The spectra of compounds **2**, **2**/Cu^{2+}, **2**/Pd^{2+} contain signals for C 1s, O 1s, N 1s, which confirms the elemental composition of all three compounds. The type of palladium signal indicates the presence of two forms of palladium, Pd 3d and Pd (0), in the structure of the powder. Additionally, a Cl 2p signal was observed in the **2**/Pd^{2+} spectrum, which corresponds to the second type of ligand at the central Pd atom in the **2**/Pd^{2+} polymer (Fig. 5c).

The complex formation of **2**/Cu^{2+} and **2**/Pd^{2+} was additionally confirmed by molecular mechanics (MMFF). Macrocycle **2** has 7396 conformations, and the one with the lowest energy molecular mechanics (MM) geometry was used as the starting point for the calculation. As a result of the study, it was shown that two fundamental models of interaction **2**/Cu^{2+} and **2**/Pd^{2+} are possible: “end-to-end” and “side-by-side” with the "end-to-end" structure four times lower in steric energy (ESI, S27).

Binding of nitroaromatic compounds

Host-guest complexation is a unique characteristic of the macrocyclic compounds. The electron rich cavity of pillar[5]arene makes it possible to form the inclusion complexes with electron-

deficient guest molecules via π-π stacking, cation-π, CH-π interactions, H-bonds, and Van der Waals forces.[56, 57] The list of potential guest molecules involves aromatic systems with electron accepting substituents, e.g., nitro derivatives of benzene, phenol and aniline.[58–60] In this respect, we have investigated the ability of macrocycle **2** and of the metallo-supramolecular coordination polymers **2**/Cu^{2+} and **2**/Pd^{2+} to form host-guest complexes with a number of nitrophenol derivatives: 2-nitrophenol (*o*-NP), 3-nitrophenol (*m*-NP), 4-nitrophenol (*p*-NP), 2,4-dinitrophenol (2,4-dNP), 2,6-dinitrophenol (2,6-dNP), and 2,4,6-trinitrophenol (2,4,6-tNP). It should be noted that functionalized pillararenes have demonstrated molecular recognition of these compounds.[22, 61, 62] Thus, Yang et al. have developed coordination polymers from decacarboxylated pillar[5]arene[63] and monocarboxylated pillar[5]arene [64] with fluorescent properties sensitive to nitroaromatic pollutants. Conjugated macrocycle polymers involving pillar[5]arene and Pd nanoparticles has been synthesized by the same group.[65] The polymer showed excellent catalytic activity in the Suzuki-Miyaura coupling reaction. However, the synthesis of similar materials on a mass scale is complicated by multistep syntheses, low yields in intermediate steps and high cost of the reagents used. As alternative, we have suggested two-step synthesis of the metallo-supramolecular coordination polymers **2**/Cu^{2+} and **2**/Pd^{2+} with good yields and based on inexpensive reagents.

The investigation of the interaction of macrocycle **2** with nitrophenol derivatives was performed by absorbance spectroscopy in methanol. The concentrations of nitrophenol derivatives were varied from 1.25 μM to 0.45 mM with the concentration of macrocycle **2** held constant at 5.0 μM. The UV-vis spectroscopy showed selectivity of **2** for 2,4-dNP and 2,6-dNP and no response to *o*-, *m*- or *p*-NP (ESI, S14-S17). The association constants (K_{ass}) were determined for the reaction **2** and the nitrophenols using the isomolar series method (ESI, S14-S17). Thus, the logK_{ass} of the

complex between the macrocycle **2** and 2,4-dNP was equal to 4.68, that for complex with 2,6-dNP - 5.63, and with 2,4,6-tNP - 2.65. The stoichiometry of the complex with 2,4-dNP was found to be 2:1 and 1:1 for other reactants (ESI, S14-S17).

Next, we studied the changes in the ^{1}H NMR spectra of 2,4-dNP and 2,4-dNP/**2**/Pd^{2+} and 2,4-dNP/**2**/Cu^{2+} (ESI, S18). Spectral changes in the systems **2**/Pd^{2+} (5×10^{-3} M)/2,4-dNP (1×10^{-2} M) and **2**/Cu^{2+} (5×10^{-3} M)/2,4-dNP (1×10^{-2} M) were the same. The intensity of 2,4-dNP aromatic proton signals in the 2/Pd^{2+}/2,4-dNP system decreased by an order of magnitude compared to the intensity of similar proton signals in the 1H NMR spectrum of 2,4-dNP. Unfortunately, significant displacements ($\Delta\delta \sim 0.1$ppm) were not observed in the comparative spectra of 2,4-dNP and **2**/Pd^{2+}/2,4-dNP, unlike classical systems based on pillar[5]arenes (ESI, S18). In this regard, we investigated a **2**/2,4-dNP system using 2D ^{1}H-^{1}H NOESY NMR spectroscopy (ESI, S19) to confirm the participation of macrocycle **2** in the interaction with 2,4-dNP. The 2D ^{1}H-^{1}H NOESY NMR spectrum of the **2**/2,4-dNP mixture in a 2:1 ratio (10^{-3} M) (ESI, S19) shows the presence of cross-peaks between the $\mathbf{H^3}$ protons (methylene groups of acetamide fragments) of macrocycle **2** and the $\mathbf{H^c}$ protons of 2,4-dinitrophenol, as well as $\mathbf{H^4}$ protons (amide fragments) of **2** and $\mathbf{H^a}$ protons of 2,4-dinitrophenol. These results confirm the ability of macrocycle **2** to form associates with 2,4-dinitrophenol.

Additional experiments were performed to confirm the specificity for recognition of nitroaromatic compounds using p-nitrotoluene, 2,4-dinitroaniline and phenol. It was shown that pillar[5]arene **2** (10^{-5}M) does not interact with any of the guests (10^{-4}M) by UV-vis spectroscopy (ESI, S18). The spectral changes were so small that it was not possible to establish the spectral characteristics of the binding and any spectral changes corresponded to the law of additivity of absorption.

Selective and efficient binding of some nitrophenol compounds made it possible to suggest an application of the obtained metallo-supramolecular coordination polymers **2**/Cu^{2+} and **2**/Pd^{2+} as sorbents for the above guest molecules. In this respect, sorption characteristics of the **2**/Cu^{2+} and **2**/Pd^{2+} polymers, which are insoluble in water, toward *o*-NP, *m*-NP, *p*-NP, 2,4-dNP, 2,6-dNP, and 2,4,6-tNP were studied. The investigation was performed with the UV-vis spectroscopy. First, the absorbance A_0 of 0.1 μg/mL nitrophenol solution was spectrophotometrically measured. Then, the sorbent (**2**/Cu^{2+} or **2**/Pd^{2+} polymers) were mixed with the nitrophenol solution for 14 hours at ambient temperature. This time was found sufficient to establish an adsorption equilibrium and no changes in the spectra caused by nitrophenol adsorption were found after this time period (ESI, S26). The saturation of the particles of the metallo-supramolecular coordination polymers **2**/Cu^{2+} and **2**/Pd^{2+} with nitrophenol was monitored spectrophotometrically until constant absorbance (A_n=const) at a certain wavelength specified for each nitrophenol.[66] Then, extraction efficiency (R, %) was calculated as a measure of adsorption capability. The value obtained depended on the sorbate nature and logK_{ass} of the reaction between the macrocycle **2** and nitrophenol. This suggested the possibility of selective adsorption of nitrophenol derivatives by the metallo-supramolecular coordination polymers **2**/Cu^{2+} and **2**/Pd^{2+}. As was shown (Figure 6), *o*-, *m*- and *p*-nitrophenols exhibit poor adsorptive activity (R = 2-23%) on the polymers **2**/Cu^{2+} and **2**/Pd^{2+}, though the association constants increased with the number of accepting groups in the sorbate molecule. The extraction efficiency increased in the range *p*-NP < *o*-NP < *m*-NP < 2,4-dNP < 2,4,6-tNP ≤ 2,6-dNP (2-46%). Most effective extracted 2,6-dNP showed the efficiency of 44 and 46% for **2**/Cu^{2+} and **2**/Pd^{2+}, respectively (Figure 6).

To compare the adsorption efficiency, activated carbon (charcoal), frequently used in industry [67-69], was chosen as a standard. under the same working conditions, the efficiency of extraction of

2.4-dNP, 2,6-dNP and 2,4,6-tNP with charcoal was tenfold lower (2-7%) than that achieved with **2**/Cu^{2+} and **2**/Pd^{2+} (32-46%) (Figure 6). The use of the macrocycle **2** as a reference material was limited by its low solubility in water.

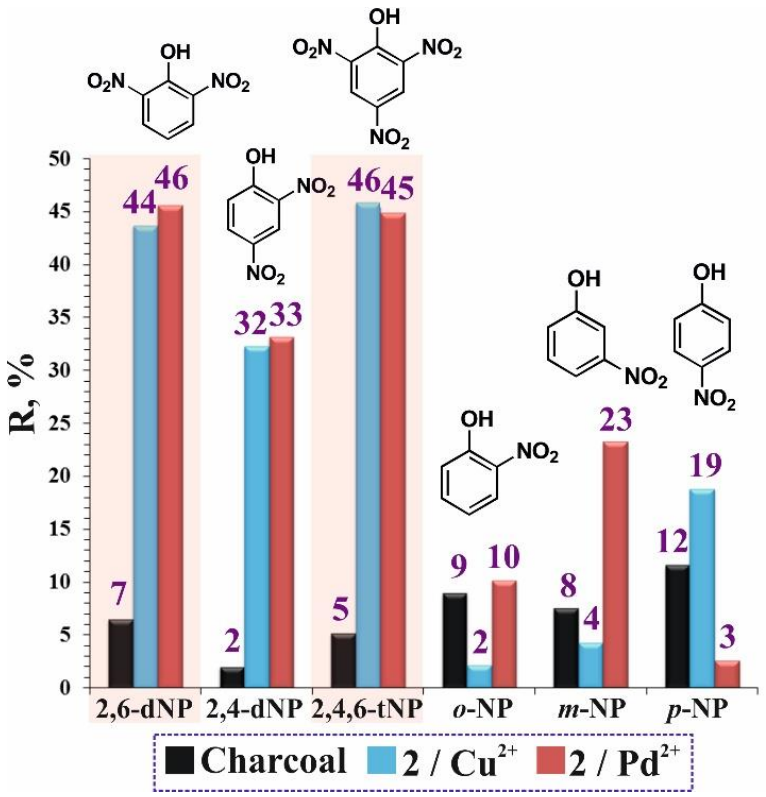

Figure 6. The efficiency of extraction (R, %) of nitrophenol derivatives (10 μg/mL) by adsorbents **2**/Cu^{2+} (10 μg/mL), **2**/Pd^{2+} (10 μg/mL) and charcoal (10 μg/mL) from water for 14 hours.

Electrochemical sensor with 2/Cu^{2+} polymer for nitrophenol determination

Selective adsorption of nitrophenols by the synthesized metallo-supramolecular coordination polymers offers attractive opportunities for development of electrochemical sensors for the determination of such compounds. To prove this concept, we have assembled electrochemical sensor with **2**/Cu^{2+} polymer as an example of such an approach. The glassy carbon electrode was

modified by drop-casting of the **2**/Cu^{2+} polymer suspension followed by its drying and washing out (see Experimental section).

It is well known, that nitroaromatic compounds can be electrochemically reduced on various electrodes [70-72]. In voltammetry, the number and position of the reduction peaks highly depends on the analyte nature and pH of the solution. Appropriate dependencies are presented in Figure 7 for various loading of the polymer on the electrode surface. On voltammograms, irreversible cathodic peak appeared between -180 and -500 mV. In some cases, a small second, poorly resolved, peak could be seen against the main reduction peak and was attributed to the redox reaction of adsorbed intermediates. Its existence and height were not been taken into account due to low reproducibility and partial overlapping with the wave of molecular oxygen reduction.

The reaction of the nitro group reduction assumes hydrogen ions are consumed so that the cathodic peak of 2,4-dNP reduction shifts with the pH increase to more negative potentials. The following experiments were performed in 0.2 M sulfuric acid. The cathodic current related to the 2,4-dNP first increased with the quantity of the **2**/Cu^{2+} polymer loaded but then slightly decreased due to partial blocking of the electrode with non-conductive polymer and increased resistance of diffusional transfer of the analyte to the electrode surface. No signals attributed to the redox activity of the **2**/Cu^{2+} polymer were found for any type of surface modification.

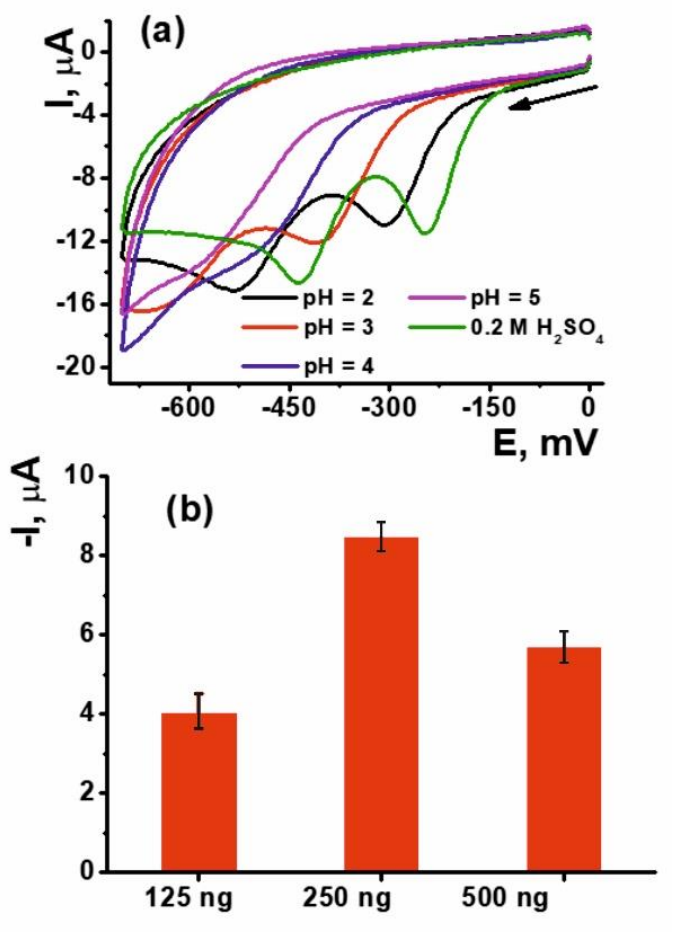

Figure 7. (a) Cyclic voltammograms of 2,4-dNP obtained with glassy carbon electrode covered with **2**/Cu^{2+} at various pH of the working buffer after incubation in 0.1 mM 2,4-dNP; (b) The 2,4-dNP reduction current at various amounts of the metallo-supramolecular coordination polymer **2**/Cu^{2+} deposited on the glassy carbon electrode. Arrow indicates the direction of the potential scanning. Scan rate was 100 mV/s.

The optimal incubation period was established for 2,4-dNP accumulation on the electrode (Figure 8). On bare glassy carbon, the adsorption of the 2,4-dNP was insignificant but in the presence of the **2**/Cu^{2+} polymer appropriate peak currents increased tenfold with the maximum at

10 min incubation. After that, the signals started decreasing probably due to influence of the nitrophenol on the structure of the supramolecular polymer and compression of the modifier layer.

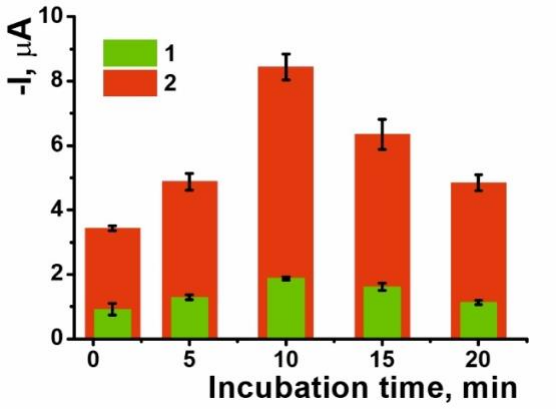

Figure 8. The dependence of the 2,4-dNP reduction peak current on the incubation period. Measurements on bare glassy carbon electrode (1) and that modified with 250 ng of **2**/Cu^{2+} polymer (2) in 0.2 M sulfuric acid, 100 mV/s. Average ± S.D. for three repetitions.

Other nitrophenols tested showed much lower accumulation in the surface layer in agreement with the range of their adsorption ability established in spectrophotometric experiment (Figure 9).

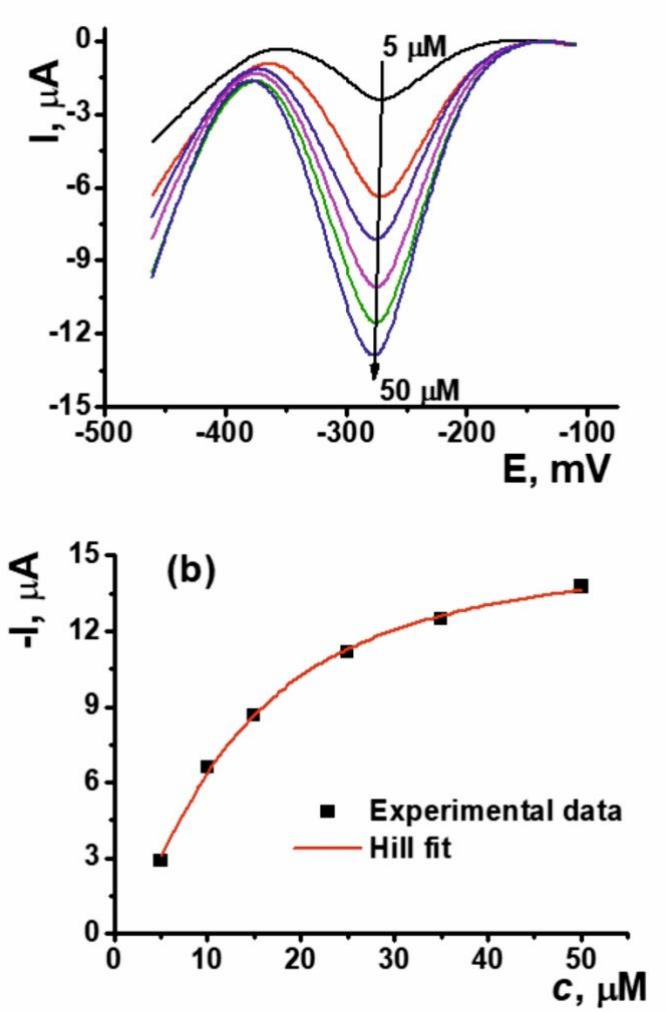

Figure 9. (a) DPV of the 2,4-dNP obtained with glassy carbon electrode modified with 250 ng of **2**/Cu^{2+} polymer in 0.2 M H_2SO_4 after 10 min incubation in 5, 10, 15, 25, 35 and 50 µM 2,4-dNP; (b) concentration regression of 2,4-dNP reduction peak current.

For determination of 2,4-dNP, differential pulse voltammetry (DPV) was used as a more sensitive method of electroanalysis. The reduction of the nitroaromatic compound was monitored by the peak current recorded at -280 mV in the concentration range from 5 to 50 µM. The dependency is appropriately non-linear due to the limiting step of analyte adsorption at the surface layer. For this reason, a nonlinear curve fit in accordance with the Hill model (Eq. 1) was used.

$$I = \frac{I_{max} c^n}{k^n + c^n}, \quad (1)$$

where I_{max} is limiting value of the peak current, μA, c is the 2,4-dNP concentration and k and n are approximation parameters. The following results of the fitting were obtained (Figure 9): I_{max} = 15.4±0.5 μA, k = 12.6±0.6, n = 1.5±0.1, R^2 = 0.9969.

Previously, Cu based metallo-organic frameworks combined with reduced graphene oxide have been successfully applied for the determination of 2,4,6-tNP over dinitro derivatives [71]. However, no information on electrochemical discrimination of dinitroaromatic compounds over mononitrophenols is available. Although the concentration range of the 2,4-dNP was quite narrow, selective determination of the dinitro derivative in the presence of mononitroaromatic compounds might be interesting to monitor waste waters and contamination control in the industrial manufacture of nitroaromatic compounds.

Conclusions

Decasubstituted pillar[5]arenes containing amidopyridine fragments have been synthesized for the first time and used to assemble metallo-supramolecular coordination polymers with the Cu^{2+} or Pd^{2+} bridging cations. All compounds obtained were characterized by ^1H and ^{13}C NMR spectroscopy, IR spectroscopy, MALDI-TOF mass-spectrometry and elemental analysis. DLS confirmed the formation of self-associates of macrocycle **2** with *p*-amidopyridine fragments in 0.1 mM solution. The associates have a hydrodynamic diameter of 120.5 nm and PDI of 0.12. By using UV-vis spectroscopy, it was shown that macrocycle **2** can form supramolecular associates with the Cu^{2+} and Pd^{2+} cations in methanol. A 2:1 stoichiometry was found and association constants ($K_{2:1}$(**2**/Pd^{2+}) = 9827072 M^{-1}, $K_{2:1}$(**2**/Cu^{2+}) = 1133170 M^{-1}) calculated by BindFit. Through interaction of **2** with Cu^{2+} and Pd^{2+} cations in methanol, metallo-supramolecular

coordination polymers **2**/Cu^{2+} and **2**/Pd^{2+} were obtained. DLS indicated the formation of monodisperse associates **2**/Cu^{2+} (PDI = 0.23) and **2**/Pd^{2+} (PDI = 0.19) with average hydrodynamic diameters of 80 and 66 nm, respectively. The formation of the metallo-supramolecular coordination polymers as gels started at 10 mM concentrations of the 2:1 **2**/Cu^{2+} and **2**/Pd^{2+} mixtures. From TEM, the structure of the gel matrix was found to consist of a regular 3D network of dense nanofibers with the filament diameter of 20 nm for **2**/Cu^{2+} and 30 nm for the **2**/Pd^{2+}. Using sol-gel methods, the **2**/Cu^{2+} and **2**/Pd^{2+} gels were transformed into amorphous powders. Retention of the regular metallo-supramolecular coordination polymer structure **2**/Cu^{2+} and **2**/Pd^{2+} was confirmed by SEM, EDS mapping and EPR, the thermostability of the products was controlled by TG/DSC. Metallo-supramolecular coordination polymers **2**/Cu^{2+} and **2**/Pd^{2+} selectivity adsorbed nitrophenols with *o-, m-* and *p*-nitrophenols are weakly adsorbed (2-23%). Increasing numbers of accepting groups in the sorbate molecule resulted in a higher extraction efficiency and an increasing association constant for the series *p*-NP < *o*-NP < *m*-NP < 2,4-dNP < 2,4,6-tNP ≤ 2,6-dNP (32-46%). This selectivity made it possible to modify an electrochemical sensor to selectively determine 2,4-dNP in aqueous solutions in the micromolar range. The results can find application in the purification of industrial waters and sensor-based monitoring of the traces of nitroaromatic compounds in the environment.

Experimental part

Safety precautions

Caution! TNP is highly explosive and should be handled carefully and in small amounts. The explosives were handled as dilute solutions using safety measures to avoid explosion.

Materials

All the reagents were purchased and used without additional purification. Dicloromethane (Merck), acetonitrile (Acros organics), trichloromethane (Merck), methanol (Merck), thionyl chloride (Merck), 2-aminopyridine (Acros Organics), 3-aminopyridine (Acros Organics), 4-aminopyridine (Acros Organics), $Cu(NO_3)_2 \cdot 3H_2O$ (Merck), $Co(NO_3)_2 \cdot 6H_2O$ (Merck), $Ni(NO_3)_2 \cdot 6H_2O$ (Merck), $Fe(NO_3)_3 \cdot 9H_2O$(Merck), $Cd(NO_3)_2 \cdot 6H_2O$ (Merck), $PdCl_2$ (Acros Organics), 2,4,6-trinitrophenol (Acros Organics), 2,4-dinitrophenol (Merck), 2,6-dinitrophenol (Acros Organics), 2-nitrophenol (Acros Organics), 3-nitrophenol (Merck), 4-nitrophenol (Merck), 4-nitrotuluene (Acros Organics), phenol (Acros Organics), 2,4-dinitroaniline (Merck), 99.8 % DMSO-d_6 (Merck)

Voltammetric measurements were performed in 0.2 M sulfuric acid, pH dependency of electrochemical characteristics was investigated in the Britton-Robinson buffer. It was prepared by dissolution of 0.1237 g of boric acid, 136 μL of 85% phosphoric acid, 115 μL of glacial acetic acid in 50 mL of deionized water followed by the pH correction with 0.2 M NaOH.

Macrocycle **1** and acyl chloride derivative of the **1** were synthesized according to the literature procedure. [33]

Methods

Synthesis of aminopyridine derivatives of pillar[5]arene

In a round-bottom flask with a magnetic stirrer 13.1 mmol of aminopyridine (2-, 3- or 4-aminopyridine) was stirred with 10 ml of anhydrous methylene chloride under cooling in an ice–salt bath (-10°C). In another flask, freshly prepared acyl chloride derivative of macrocycle **1** (0.3 g, 0.218 mmol) was dissolved in 10 mL of anhydrous methylene chloride and transferred to an

addition funnel. Then, within 15 min, a solution of macrocycle **1** acid chloride was dropped to the aminopyridine solution while cooling in an ice bath (-10°C). Next, the dropping funnel was removed, blown out with argon and closed with a glass stopper. The reaction mixture was stirred for 72 h at -10°C. The resulting solution was washed three times with 30 mL of distilled water. The organic layer was separated and evaporated to dryness on a rotary evaporator. The target products were isolated by recrystallization from the water with the yields of 77, 61 and 71% for the macrocycle**s 2-4** (Fig. 1), respectively.

Synthesis of metallo-supramolecular coordination polymers 2/Cu^{2+}, 2/Pd^{2+}

0.017 g of macrocycle **2** were dissolved in 1 mL of methanol (c = 1×10^{-2} M) under ultrasonic treatment, then 1 mL of a solution of a metal salt ($Cu(NO_3)_2$, $PdCl_2$) in methanol (c = 1×10^{-2} M) were added. The resulting gel-like precipitate was thermostated at 25°C for 20 minutes, then methanol was separated from the unit by centrifugation. The obtained polymer particles were washed three times with 10 mL of methanol and centrifuged. Then the precipitate was dried in vacuum under reduced pressure.

Electrochemical measurements

All the electrochemical measurements were performed at ambient temperature in the non-thermostated three-electrode cell with glassy carbon working electrode (2 mm in diameter), Ag / AgCl / 3 M KCl reference electrode and Pt rod as auxiliary electrode in 1 mL of phosphate buffer or sulfuric acid. The voltammetric experiments in direct current or differential pulse voltammetry mode were performed with electrochemical analyzer CHI 440B (CH Instruments, Inc., TX, USA). For electrode modification, it was first mechanically polished and sonicated for 1

min in deionized water and 1 min in ethanol. Then, the electrode was dried at ambient temperature and drop-casted with an aliquot of the suspension of metallo-supramolecular coordination polymer **2**/Cu^{2+} in DMF prepared by 30 min. sonication. After that, the electrode was dried for 30 min., washed with water and used for voltammetric measurements.

Characterization

^{1}H NMR, ^{13}C NMR spectra were obtained on a Bruker Avance-400 spectrometer (^{13}C - 100 MHz and ^{1}H - 400 MHz). Chemical shifts were determined against the signals of residual protons of deuterated solvent (DMSO-d_6, D_2O). The concentration of sample solutions was 3-5 %. Attenuated total internal reflectance IR spectra were recorded with Spectrum 400 (Perkin Elmer) Fourier spectrometer. The IR spectra from 4000 to 400 cm^{-1} were considered in this analysis. The spectra were measured with 1 cm^{-1} resolution and 64 scans co-addition. Elemental analysis was performed with Perkin Elmer 2400 Series II instrument. Mass spectra (MALDI-TOF) were recorded on Ultraflex III mass spectrometer in the 4-nitroaniline matrix. Melting points were determined using the Boetius Block apparatus. Powder X-ray diffraction (PXRD) analyses of samples were carried out over the 2θ range of 5° to 70° on a PANalytical B.V. Empyrean powder diffractometer. The study of Cu(II)-containing metallo-supramolecular aggregates was carried out on an electron paramagnetic resonance (EPR) spectrometer Bruker ESP-300, operating at X-band (9.6 GHz) microwave frequency in the temperature range T = 20-300K. Additional control of the purity of compounds and monitoring of the reaction were carried out by thin-layer chromatography using Silica G, 200 μm plates, UV 254. UV-vis spectra were recorded using the Shimadzu UV-3600 spectrometer; the cell thickness was 1 cm, slit width - 1 nm. Deionized water with a resistivity

>18.0 MΩ cm was used to prepare the solutions. Deionized water was obtained from a Millipore-Q purification system.

Spectroscopic studies

The absorption spectra of the mixtures of macrocycle **2-4** (1×10^{-5} - 5×10^{-5} M) with $Fe(NO_3)_2$, $Ni(NO_3)_2$, $Co(NO_3)_2$, $Cd(NO_3)_2$, $Cu(NO_3)_2$, $PdCl_2$, 2,4,6-tNP, 2,4-dNP, 2,6-dNP, *o*-, *m*- and *p*-NP were recorded after mixing the solutions at 298 K. The 1×10^{-5} - 5×10^{-5} M solution of the guest ($Cu(NO_3)_2$, $PdCl_2$, 2,4,6-tNP, 2,4-dNP, 2,6-dNP (50, 75, 100, 150, 300, 400, 500, 600, 700, 900, 1200, 1500, 1800, 2100, 2400 and 2700 μL, 1×10^{-5}-5×10^{-5} M) in methanol was added to 300 μL of the solution of macrocycle **2-4** (1×10^{-5} - 5×10^{-5} M) in methanol and diluted to final volume of 3 mL with methanol. The UV spectra of the solutions were then recorded. The stability constant of complexes were calculated as described below. Three independent experiments were carried out for each series. Student's *t*-test was applied in statistical data processing. Experiment was carried out according to the literature method. Stoichiometry of complexes was determined by Job's plot.

Transmission electron microscopy (TEM)

TEM analysis of samples was carried out using the JEOL JEM 100CX II transmission electron microscope. For sample preparation, 10 μL of the suspension 10^{-3}-10^{-5} M were placed on the Formvar™/carbon coated 3 mm nickel grid, which was then dried at room temperature. After complete drying, the grid was placed into the transmission electron microscope using special holder for microanalysis. Analysis was held at the accelerating voltage of 80 kV in SEM mode by Carl Zeiss Merlin microscope.

Simultaneous thermogravimetry and differential scanning calorimetry (TG–DSC)

TG–DSC was performed on a Netzsch Jupiter STA 449 C Jupiter analyzer in 40-μL platinum crucibles with a cap having a 0.5-mm hole at constant heating rates (10 and 4 deg/min; heating range 311–783 K) in dynamic argon atmosphere, flow rate 20 mL/min, atmospheric pressure; sample weight 10–20 mg.

XPS measurements

XPS measurements were performed in a UHV chamber (base pressure ~ 5×10^{-10} mbar) equipped with Al Kα X-ray source operated at 12.5 kV and 250 W, and a Phoibos 150 hemispherical energy analyzer (all from SPECS GmbH). Pass energy of 100 eV (step size of 1 eV) was used for wide range scans (survey), while 20 eV pass energies (step size of 0.1 eV, 25 scans) were used for high resolution measurements. Peak shifts due to any apparent charging were calibrated with the carbon C1s peak set to 284.8 eV. XPS spectra registered from experimental samples were analyzed with the CasaXPS software (Casa Software Ltd). The elemental concentrations were retrieved from the area of the detected peaks for each element using sensitivity factors (provided by instrument manufacturer), respectively.

Dynamic light scattering (DLS)

The particle size and zeta potential ware determined by the Zetasizer Nano ZS instrument at 20 °C. The instrument contains 4 mW He-Ne laser operating at a wave length of 633 nm and incorporated noninvasive backscatter optics (NIBS). The measurements were performed at the detection angle of 173° and the software automatically determined the measurement position within the quartz cuvette. The 1×10^{-3} - 1×10^{-5} M methanol solutions of the **2**, metal salt ($Cu(NO_3)_2$ or $PdCl_2$) and macrocycle **2** with metal cation (Cu^{2+}/ Pd^{2+}) complex were prepared. The

concentration ratio of macrocycle **2** and metal cations in complexes was 10:1, 5:1, 2:1, 1:1, 1:2, 1:5, 1:10. The experiments were carried out for each solution in triplicate.

Adsorption of nitrophenol derivatives

0.00010 g of the sample (**2/Cu^{2+}, 2/Pd^{2+}**) was mixed with 10 ml of sorbate (c = 1×10^{-5} M) in water for 24 h at room temperature. Then the aqueous solution over the sorbent layer was filtered through a nylon filter (0.45 μm). The residual concentration of the solute in the filtrate was measured using a UV spectrometer (using the maximum absorption at a specific wavelength for each aromatic substance: 2,4,6-tNP = 355 nm, *o*-NP = 282 nm, *m*-NP = 280 nm, *p*-NP = 271 nm, 2,4-dNP = 358 nm and 2,6-dNP = 413 nm). The time to reach full saturation of the sorbent was determined by studying the kinetics of sorption by stirring using a magnetic stirrer systems "sorbate-sorbent" at a temperature of 25±2°C. After sorption, samples of the solutions were taken at different time intervals (30 min, 1 hour, 2 hours, 3 hours, 4 hours, 24 hours, 48 hours), filtered through a filter with a pore size of 0.45 μm. Electronic absorption spectra for these aqueous solutions were recorded and it was found that after 24 h the optical density of the analyte solution remained practically unchanged, and this corresponded to the maximum saturation of the sorbent. The efficiency of extracting the adsorbate from the solution, R (%), was calculated using the following equation: R = (c_o-c_a) × 100% / c_o. According to the Bouguer-Lambert-Beer law A ~ c, that is: R = (A_o - A_a) × 100% / A_o, where c_o and c_a (mg/L) are the initial and residual adsorbate concentrations, respectively, A_o and A_a are the optical densities of the solution before and after sorption of the sorbate, respectively. The experiments were carried out for each solution in triplicate.

Detailed information of physical-chemical characterization is presented in Electronic Supporting Information (ESI).

ASSOCIATED CONTENT

Structural characterization, figures with ^{1}H, ^{13}C NMR, FT-IR, MALDI-TOF spectra of all compounds synthesized, the detailed experimental results for the determination of the association constants between the hosts and the guests are available free of charge via the Internet at http:// pubs.acs.org. (PDF)

AUTHOR INFORMATION

Corresponding Author

Ivan I. Stoikov

E-mail: Ivan.Stoikov@mail.ru

Fax: +7-8432-752253

Tel: +7-8432-337463

Author Contributions

The manuscript was written through contributions of all authors. All authors have given approval to the final version of the manuscript.

Funding Sources

The work was supported by the Russian Science Foundation (Grant No 17-13-01208).

Notes

The authors declare no competing financial interest

ACKNOWLEDGMENTS

The investigation of structure of the compounds by NMR spectroscopy was carried out within the framework of the grant of the President of the Russian Federation for state support of leading scientific schools of the Russian Federation (NSh-2499.2020.3).

A.A. Rodionov acknowledges support of the state subsidy in the sphere of scientific activity for Kazan Federal University (proposal 0671-2020-0051) for possibility to carry out EPR measurements at low temperatures.

ABBREVIATIONS

DFRL, dark field reflected light mode; DLS, dynamic light scattering; DMF, dimethylformamide; DMSO, dimethyl sulfoxide; EPR, electron paramagnetic resonance; FT-IR, Fourier-transform infrared spectroscopy; PDI, polydispersity index; PXRD, Powder X-Ray Diffraction; SEM, scanning electron microscopy; TEM, transmission electron microscopy; TGA-DTA/DSC, Simultaneous thermogravimetry and differential scanning calorimetry; UV-vis spectroscopy, ultraviolet spectroscopy.

REFERENCES

1. Lehn, J. M. Supramolecular polymer chemistry—scope and perspectives. *Polym. Int.* **2002**, *51*, 825-839.

2. Dobrawa, R.; Würthner, F. Metallosupramolecular approach toward functional coordination polymers. *J. Polym. Sci. Pol. Chem*. **2005**, *43*, 4981-4995.

3. Zhang, J. P.; Huang, X. C.; Chen, X. M. Supramolecular isomerism in coordination polymers. *Chem. Soc. Rev*. **2009**, *38*, 2385-2396.

4. Pai, S.; Schott, M.; Niklaus, L.; Posset U.; Kurth, D. G. A study of the effect of pyridine linkers on the viscosity and electrochromic properties of metallo-supramolecular coordination polymers. *J. Mater. Chem. C*. **2018**, *6*, 3310-3321.

5. Lou, X. Y.; Yang, Y. W.; Manipulating aggregation-induced emission with supramolecular macrocycles. *Adv. Opt. Mater.* **2018**, *6*, 1800668-1800693.

6. Li, H. Q.; Ding, Z. Y.; Pan, Y.; Liu, C. H.; Zhu, Y. Y. Fluorescence tuning of Zn (II)-based metallo-supramolecular coordination polymers and their application for picric acid detection. *Inorg. Chem. Front*. **2016**, *3*, 1363-1375.

7. Winter, A.; Schubert, U. S. Synthesis and characterization of metallo-supramolecular polymers. *Chem. Soc. Rev.* **2016**, *45*, 5311-5357.

8. Zheng, B.; Hou, Y.; Gao, L.; Zhang, M. Luminescent Metallo-Supramolecular Polymers. *Chin. J. Chem.* **2019**, *37*, 843-854.

9. Verbitskiy, E. V.; Rusinov, G. L.; Chupakhin, O. N.; Charushin, V. N. Design of fluorescent sensors based on azaheterocyclic push-pull systems towards nitroaromatic explosives and related compounds: A review. *Dyes Pigm.* **2020**, *180*, 108414-108433.

10. Tiwari, J.; Tarale, P.; Sivanesan, S.; Bafana, A. Environmental persistence, hazard, and mitigation challenges of nitroaromatic compounds. *Environ. Sci. Pollut. R*. **2019**, *26*, 28650-28667.

11. Ding, Z.; Li, H.; Gao, W.; Zhang, Y.; Liu C.; Zhu, Y. Detection of picric acid by terpy-based metallo-supramolecular fluorescent coordination polymers in aqueous media. *Chin. J. Chem.* **2017**, *35*, 447-456.

12. Wang, R.; Liu, X.; Huang, A.; Wang, W.; Xiao, Z.; Zhang, L.; Dai, F.; Sun, D. Unprecedented solvent-dependent sensitivities in highly efficient detection of metal ions and nitroaromatic compounds by a fluorescent barium metal–organic framework. *Inorg. Chem.* **2016**, *55*, 1782-1787.

13. Zhang, N.; Li, B.; Wang, X.; Liu, D.; Han, X.; Bai, F.; Xing, Y. High-efficiency fluorescent probe constructed by triazine polycarboxylic acid for detecting nitro compounds. *Inorg. Chim. Acta*. **2020**, *507*, 119591-119600.

14. Zhang, L.; Sun, L.; Li, X.; Tian, Y.; Yuan, G. Five 8-hydroxyquinolinate-based coordination polymers with tunable structures and photoluminescent properties for sensing nitroaromatics. *Dalton T.* **2015**, 44, 401-410.

15. Noor, A.; Moratti, S. C.; Crowley, J. D. Active-template synthesis of "click" [2]rotaxane ligands: self-assembly of mechanically interlocked metallo-supramolecular dimers, macrocycles and oligomers. *Chem. Sci.* **2014**, *5*, 4283-4290.

16. Ovsyannikov, A.; Solovieva, S.; Antipin, I.; Ferlay, S. Coordination polymers based on calixarene derivatives: Structures and properties. *Coordin. Chem. Rev*. **2017**, *352*, 151-186.

17. Liu, Y.; Zhao, Y. L.; Zhang, H. Y.; Song, H. B. Polymeric rotaxane constructed from the inclusion complex of β-cyclodextrin and 4,4′-dipyridine by coordination with Nickel (II) ions. *Angew. Chem. Int. Ed*. **2003**, *42*, 3260-3263.

18. Facciotti, C.; Saggiomo, V.; Bunschoten, A.; Fokkink, R.; Ten Hove, J. B.; Wang, J.; Velders, A. H. Cyclodextrin-based complex coacervate core micelles with tuneable supramolecular host–guest, metal-to-ligand and charge interactions. *Soft matter*. **2018**, *14*, 9542-9549.

19. Li, F. Z.; Mei, L.; Hu, K. Q.; Yu, J. P.; An, S. W.; Liu, K.; Chai, Z.; Liu, N.; Shi, W. Q. Releasing metal-coordination capacity of cucurbit[6]uril macrocycle in pseudorotaxane ligands for the construction of interwoven uranyl–rotaxane coordination polymers. *Inorg. Chem.* **2018**, *57*, 13513-13523.

20. Fowler, D. A.; Mossine, A. V.; Beavers, C. M.; Teat, S. J.; Dalgarno S. J.; Atwood, J. L. Coordination polymer chains of dimeric pyrogallol[4]arene capsules. *J. Am. Chem. Soc*. **2011**, *133*, 11069-11071.

21. Zhao, W.; Qiao, B.; Tropp, J.; Pink, M.; Azoulay J. D.; Flood, A. H. Linear Supramolecular polymers driven by anion–anion dimerization of difunctional phosphonate monomers inside cyanostar macrocycles. *J. Am. Chem. Soc*. **2019**, *141*, 4980-4989.

22. Li, Y. F.; Li, Z.; Lin, Q.; Yang, Y. W. Functional supramolecular gels based on pillar[n]arene macrocycles. *Nanoscale*. **2020**, *12*, 2180-2200.

23. Fa, S.; Kakuta, T.; Yamagishi, T. A.; Ogoshi, T. One-, Two-, and three-dimensional supramolecular assemblies based on tubular and regular polygonal structures of pillar[n]arenes. *CCS Chem.* **2019**, *1*, 50-63.

24. Shurpik, D. N.; Sevastyanov, D. A.; Zelenikhin, P. V.; Subakaeva, E. V.; Evtugyn, V. G.; Osin, Y. N.; Cragg, P. J.; Stoikov, I. I. Hydrazides of glycine-containing decasubstituted pillar[5]arenes: synthesis and encapsulation of floxuridine. *Tetrahedron let*. **2018**, *59*, 4410-4415.

25. Shurpik, D. N.; Stoikov, I. I. Covalent assembly of tris-pillar[5]aren. *Russ. J. Gen. Chem*. **2016**, *86*, 752-755.

26. Shurpik, D. N.; Mostovaya, O. A.; Sevastyanov, D. A.; Lenina, O. A.; Sapunova, A. S.; Voloshina, A. D.; Petrov, K. A.; Kovyazina, I. V.; Cragg, P. J.; Stoikov, I. I. Supramolecular neuromuscular blocker inhibition by a pillar[5]arene through aqueous inclusion of rocuronium bromide. *Org. Biomol. Chem*. **2019**, *17*, 9951-9959.

27. Yakimova, L. S.; Shurpik, D. N.; Makhmutova, A. R.; Stoikov, I. I. Pillar[5]arenes bearing amide and carboxylic groups as synthetic receptors for alkali metal ions. *Macroheterocycles*. **2017**, *10*, 226-232.

28. Shurpik, D. N.; Sevastyanov, D. A.; Zelenikhin, P. V.; Padnya, P. L.; Evtugyn, V. G.; Osin, Y. N.; Stoikov I. I. *Beilstein J. Nanotech*. **2020**, *11*, 421-431.

29. Ogoshi, T.; Hasegawa, Y.; Aoki, T.; Ishimori, Y.; Inagi, S.; Yamagishi T. *Macromolecules*. **2011**, *44*, 7639-7644.

30. Smolko, V. A.; Shurpik, D. N.; Shamagsumova, R. V.; Porfireva, A. V.; Evtugyn, V. G.; Yakimova, L. S.; Stoikov, I. I.; Evtugyn, G. A. Electrochemical behavior of pillar[5]arene on glassy carbon electrode and its interaction with Cu^{2+} and Ag^{+} ions. *Electrochim. Acta.* **2014**, *147*, 726-734.

31. Shamgsumova, R. V.; Shurpik, D. N.; Evtugyn, V. G.; Stoikov, I. I.; Evtugyn, G. A. Electrochemical determination of malathion on an acetylcholinesterase-modified glassy carbon electrode. *Anal. Lett.* **2018**, *51*, 1911-1926.

32. Kuzin, Y.; Kappo, D.; Porfireva, A.; Shurpik, D.; Stoikov, I.; Evtugyn, G.; Hianik, T. Electrochemical DNA sensor based on carbon black-poly (neutral red) composite for detection of oxidative DNA damage. *Sensors*. **2018**, *18*, 3489-3503.

33. Shurpik, D. N.; Padnya, P. L.; Basimova, L. T.; Evtugin, V. G.; Plemenkov, V. V.; Stoikov, I. I. Synthesis of new decasubstituted pillar[5]arenes containing glycine fragments and their interactions with Bismarck brown Y. *Mendeleev Commun*., **2015**, *6*, 432-434.

34. Stoikov, I. I.; Zhukov, A. Yu.; Agafonova, M. N.; Sitdikov, R. R.; Antipinn, I. S.; Konovalov, A. I. p-tert-Butylthiacalix[4]arenes functionalized at the lower rim by o-, m-, p-amido and o-, m-, p-(amidomethyl) pyridine fragments as receptors for α-hydroxy-and dicarboxylic acids. *Tetrahedron*. **2010**, *66*, 359-367.

35. Kumar, P.; Gupta, R. The wonderful world of pyridine-2, 6-dicarboxamide based scaffolds. *Dalton Trans.* **2016**, *45*, 18769-18783.

36. Venkataramanan, N. S.; Suvitha, A.; Vijayaraghavan, A.; Thamotharan, S. Investigation of inclusion complexation of acetaminophen with pillar[5]arene: UV–Vis, NMR and quantum chemical study. *J. Mol. Liq.* **2017**, *241*, 782-791.

37. Gawron, E. L.; Hira, S. M.; Josowicz, M.; Janata, J. Effects of Palladium (II) Chlorocomplex Speciation on the Controlled Interaction with a Polyaniline Film in Acid. *Langmuir.* **2017**, *33*, 11930-11935.

38. Hibbert, D. B.; Thordarson, P. The death of the Job plot, transparency, open science and online tools, uncertainty estimation methods and other developments in supramolecular chemistry data analysis. *Chem. Commun.* **2016**, *52*, 12792-12805.

39. Bindfit; http://supramolecular.org.

40. Weng, W.; Beck, J. B.; Jamieson, A. M.; Rowan, S. J. Understanding the mechanism of gelation and stimuli-responsive nature of a class of metallo-supramolecular gels. *J. Am. Chem. Soc.* **2006**, *128*, 11663-11672.

41. Bueken, B.; Van Velthoven, N.; Willhammar, T.; Stassin, T.; Stassen, I.; Keen, D. A.; Baron, G. V.; Denayer, J. F. M.; Ameloot, R.; Bals, S.; De Vos, D.; Bennett, T. D. Gel-based morphological design of zirconium metal–organic frameworks. *Chem. Sci.* **2017**, *8*, 3939-3948.

42. Shifrina, Z. B.; Matveeva V. G.; Bronstein, L. M. Role of polymer structures in catalysis by transition metal and metal oxide Nanoparticle Composites. *Chem. Rev.* **2020**, *120*, 1350-1396.

43. Lan, S.; Yang, X.; Shi, K.; Fan, R.; Ma, D. Pillarquinone-based porous polymer for a highly-efficient heterogeneous organometallic catalysis. *ChemCatChem*, **2019**, *11*, 2864-2869.

44. Li, H.; Yang, Y.; Xu, F.; Liang, T.; Wen, H.; Tian, W. Pillararene-based supramolecular polymers. *Chem. Commun*. **2019**, *55*, 271-285.

45. Tian, T.; Zeng, Zh.; Vulpe, D.; Casco, M. E.; Divitini, G.; Midgley, P. A.; Silvestre-Albero, J.; Tan, J.-Ch.; Moghadam, P. Z.; Fairen-Jimenez, D. A sol–gel monolithic metal–organic framework with enhanced methane uptake. *Nature Materials*. **2018**, *17*, 174-179.

46. Anderegg, G.; Wanner, H. Pyridine derivatives as complexing agents. XIII. The stability of the palladium (II) complexes with pyridine, 2,2′-bipyridyl, and 1,10-phenanthroline. *Inorg. Chim. Acta*. **1986**, *113*, 101-108.

47. Liu, Y.; Guo, J. H.; Dao, X. Y.; Zhang, X. D.; Zhao, Y.; Sun, W. Y. Coordination polymers with a pyridyl–salen ligand for photocatalytic carbon dioxide reduction. *Chem. Commun.* **2020**, *56*, 4110-4113.

48. Das, K.; Mendiratta, S.; Datta, A.; Gajewska, M. J.; Garribba, E.; Akitsu, T.; Sinha, C. A New CuII coordination polymer: structural elucidation, EPR and sensing studies for detection of volatile organic solvents. *ChemistrySelect*. **2016**, *1*, 2192-2198.

49. Deshmane, V.G.; Abrokwah, R.Y.; Kuila, D. Synthesis of stable Cu-MCM-41 nanocatalysts for H2 production with high selectivity via steam reforming of methanol. *Intern. J. Hydrogen Energy*. **2015**, *40*, 10439-10452.

50. Poppl, A.; Kunz, S.; Himsl, D.; Hartmann, M. CW and Pulsed ESR Spectroscopy of Cupric Ions in the Metal− Organic Framework Compound Cu3 (BTC) 2. *J. Phys. Chem. C*. **2008**, *112*, 2678-2684.

51. Gabbasov, B.; Gafurov, M.; Starshova, A.; Shurtakova, D.; Murzakhanov, F.; Mamin, G.; Orlinskii, S. *J. Magn. Magn. Mater.* **2019**, *470*, 109-117.

52. Deshmane, V. G.; Abrokwah, R. Y.; Kuila, D. Synthesis of stable Cu-MCM-41 nanocatalysts for H_2 production with high selectivity via steam reforming of methanol. *Intern. J. Hydrogen Energy*. **2015**, *40*, 10439-10452.

53. Kunishita, A.; Ishimaru, H.; Nakashima, S.; Ogura, T.; Itoh, Sh. Reactivity of mononuclear alkylperoxo copper (II) complex. O−O bond cleavage and C− H bond activation. *J. Am. Chem. Soc.* **2008**, *130*, 4244-4245.

54. Garribba, E.; Micera, G. The determination of the geometry of Cu (II) complexes: an EPR spectroscopy experiment. *J. Chem. Educ.* **2006**, *83*, 1229-1232.

55. Jiang, Yi.; Huang, J.; Kasumaj, B.; Jeschke, G.; Hunger, M.; Mallat, T.; Baiker, A. Adsorption− desorption induced structural changes of Cu-MOF evidenced by solid state NMR and EPR spectroscopy. *J. Am. Chem. Soc.* **2009**, *131*, 2058-2059.

56. Fang, Y.; Deng, Y.; Dehaen, W. Tailoring pillararene-based receptors for specific metal ion binding: From recognition to supramolecular assembly. *Coord. Chem. Rev*. **2020**, *415*, 213313-213350.

57. Li, E.; Zhou, Y.; Zhao, R.; Jie, K.; Huang, F. Dihalobenzene shape sorting by nonporous adaptive crystals of perbromoethylated pillararenes. *Angew. Chem. Int. Ed. Engl*. **2019**, *58*, 3981-3985.

58. Yang, L.; Tan, X.; Wang, Z.; Zhang, X. Supramolecular polymers: historical development, preparation, characterization, and functions. *Chem. Rev*. **2015**, *115*, 7196-7239.

59. Jie, K.; Zhou, Y.; Li, E.; Huang, F. Nonporous adaptive crystals of pillararenes. *Acc. Chem. Res.* **2018**, *51*, 2064-2072.

60. Shurpik, D. N.; Yakimova, L. S.; Gorbachuk, V. V.; Sevastyanov, D. A.; Padnya, P. L.; Bazanova O. B.; Stoikov, I. I. Hybrid multicyclophanes based on thiacalix[4]arene and pillar[5]arene: Synthesis and influence on the formation of polyaniline. *Org. Chem. Front.* **2018**, *5*, 2780-2786.

61. Yao, Y.; Xue, M.; Chen, J.; Zhang, M.; Huang, F. An amphiphilic pillar[5]arene: synthesis, controllable self-assembly in water, and application in calcein release and TNT adsorption. *J. Am. Chem. Soc.* **2012**, *134*, 15712-15715.

62. Xiaoa, T.; Wang, L. Recent advances of functional gels controlled by pillar[n]arene-based host–guest interactions. *Tetrahedron Lett.* **2018**, *13*, 1172-1182.

63. Li, X. S.; Li, Y. F.; Wu, J. R.; Lou, X. Y.; Han, J.; Qin, J.; Yang, Y. W. A color-tunable fluorescent pillararene coordination polymer for efficient pollutant detection. *J. Mater. Chem. A.* **2020**, *8*, 3651-3657.

64. Wu, M. X.; Yang, Y. W. A fluorescent pillarene coordination polymer. *Polym. Chem.* **2019**, *10*, 2980-2985.

65. Li, Z.; Li, X.; Yang, Y. W. Conjugated Macrocycle Polymer Nanoparticles with Alternating Pillarenes and Porphyrins as Struts and Cyclic Nodes. *Small*. **2019**, *15*, 1805509-1805519.

66. Yakimova, L. S.; Ziatdinova, R. V.; Evtugyn, V. G.; Rizvanov, I. K.; Stoikov, I. I. Hybrid thiacalix[4]arene/SiO_2 nanoparticles: synthesis and selective adsorption of aniline and phenol nitro derivatives. *Russ. Chem. Bull.* **2016**, *65,* 1053-1060.

67. Tang, D.; Zheng, Zh.; Lin, K.; Luan, J.; Zhang, J. Adsorption of p-nitrophenol from aqueous solutions onto activated carbon fiber. *J. Hazard. Mater.* **2007**, *143*, 49-56.

68. Zhang, B.; Feng, L.; Wu, T.; Sun, D.; Li, Y. Adsorption of p-nitrophenol from aqueous solutions using nanographite oxide. *Colloids Surf. A: Physicochem. Eng. Aspects*. **2015**, *464*, 78-88.

69. Snoeyink, V. L.; Weber, W. J. Jr.; Mark, H. B. Jr. Sorption of phenol and nitrophenol by active carbon. *Environ. Sci. Technol*. **1969**, *3*, 918-926.

70. Rumlova, T.; Kabátová, A.; Fojta, M.; Barek, J. Determination of 2-nitrophenol using carbon film electrode. *Monatsh. Chem.* **2015**, *147*, 173-179.

71. Wang, Y.; Cao, W.; Wang, L.; Zhuang, Q.; Ni, Y. Electrochemical determination of 2,4,6-trinitrophenol using a hybrid film composed of a copper-based metal organic framework and electroreduced graphene oxide. *Microchim. Acta* **2018**, *185*, 315.

72. Lima, A. P.; Almeida, P. L. M. R.; Sousa, R. M. F.; Richter, E. M.; Nossol, E.; Munoz, R. A. A. Effect of alumina supported on glassy-carbon electrode on the electrochemical reduction of 2,4,6-trinitrotoluene: A simple strategy for its selective detection. *J. Electroanal. Chem*. **2019**, *851*, 113385.

BRIEF ABSTRACT

Decasubstituted pillar[5]arenes containing amidopyridine fragments were synthesized. These compounds are capable of forming metal-supramolecular coordination polymers. These polymers in an electrochemical sensor recognize nitrophenols in water.

For Table of Contents only

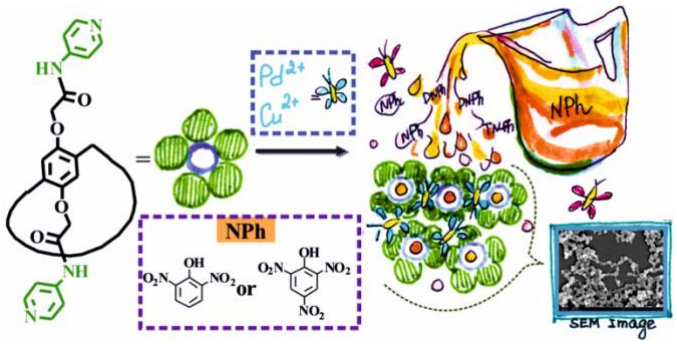
HN
O
O
O
O
NH
N
N
=
Pd2+
Cu2+
NPh
OH
O2N
NO2
or
NO2
NPh
SEM Image